Real-time Iris Segmentation based on Image Morphology

Sambit Bakshi
National Institute of Technology, Rourkela
Odisha, India
sambitbaksi@gmail.com

Hunny Mehrotra
National Institute of Technology, Rourkela
Odisha, India
hunny@nitrkl.ac.in

Dr. Banshidhar Majhi
College of Computer Science,
King Khalid University,
Saudi Arabia *
bmajhi@nitrkl.ac.in

ABSTRACT

This paper introduces an efficient iris segmentation approach for unconstrained images. Proposed technique is robust to occlusion, specular reflection, variation in illumination and non-centered gaze. For pupil localisation, the input iris image is binarised using an adaptive threshold determined based on number of connected components. Further, pupil center and radius are obtained using spectrum image based approach. The proposed technique performs accurately (>97%) with low computation (<0.4 seconds/image). It has been observed that the proposed approach can be deployed to real-time biometric systems where time as well as accuracy cannot be compromised.

Categories and Subject Descriptors

I.4.6 [**Image Processing and Computer Vision**]: Segmentation—*Edge and feature detection, Pixel classification, Region growing, partitioning*; I.4.10 [**Image Processing and Computer Vision**]: Image Representation—*Morphological*

General Terms

Security and Experimentation

Keywords

Iris Segmentation, Adaptive Threshold, Connected Components, Spectrum Image and Circular Hough Transform

1. INTRODUCTION

Iris is one of the most trusted biomtric authentications due to its accuracy, reliability and speed. The highly detailed random patterns from the iris are acquired from some distance to have real-time high confidence recognition of an individual [1]. The acquired iris image is preprocessed for localisation of inner pupil and outer iris boundary that are presumed to be concentric circular. Localised iris is used for feature extraction and matching. As localisation is the primitive operation, any failure compromises performance of the subsequent process.

There are several issues to be handled for sengmenting iris. Firstly, static threshold fails to binarize iris image for varying illumination. Secondly, iris occlusion by eyelids and eyelashes degrades the performance of localisation module. Thirdly, during image acquisition the spot of light creates specular highlights on pupil which adds noise to input and hinder localisation. Lastly, the gaze of an individual may not be centered. Such images are usually acquired in non-cooperative environment. The minimum value of mean intensity of a grid in iris image ihas been taken as threshold for binarizing the pupil [2] as shown in Figure 1, but it fails due to specular highlights. In the proposed paper, a robust iris segmentation approach has been developed that performs well for aforementioned issues. The detailed description of steps involved are given in Section 2. For accurate pupil detection, an adaptive threshold is obtained from input iris image as given in Section 2.1. The hole filled binary image is used for finding pupil boundary using spectrum image (Section 2.2). Section 2.3 outlines the approach to find outer iris boundary. Experimental results for the proposed approach are given in Section 3.

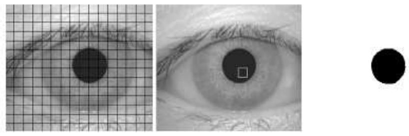

Figure 1: Binarization using adaptive threshold [2]

2. PROPOSED IRIS SEGMENTATION

Iris segmentation comprises finding the inner pupil and outer iris boundary. The annular region lying between the two boundaries is considered for feature extraction. In this paper an efficient and fast iris segmentation approach is proposed. This approach takes an input iris image and finds an adaptive threshold for pupil detection. The pupil boundary is obtained using spectrum image based approach. Finally iris boundary is found using traditional homocentric circular summation of intensities. The detailed description of steps involved are explained below:

*Dr. Banshidhar Majhi is presently on leave from National Institute of Technology Rourkela, Odisha, India

2.1 Adaptive Thresholding

Pupil is darkest region in the eye with almost circular shape. Appropriate threshold helps to find the region of interest containing pupil. Static value of threshold may fail for different images taken under varying illumination conditions [2]. In the proposed paper an effort has been made to adaptively determine the value of threshold. It has been empirically observed that the highest intensity value contributing to pupil neither exceeds $high_\tau$ (0.5 of highest grayscale value) nor drops beyond low_τ (0.1 of highest grayscale value). To find adaptive threshold, binary images are obtained iteratively for range of thresholds (τ) between low_τ and $high_\tau$ with increment of $step_\tau$ (0.05 of highest grayscale value). Parameters are optimized based on trade off between computational complexity and accuracy.

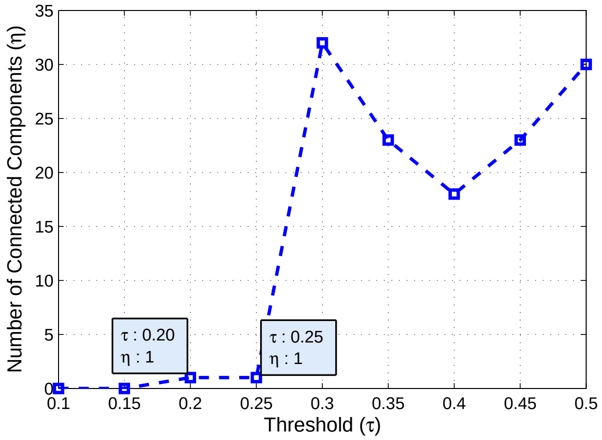

Figure 2: Relationship between τ and η

The binary images obtained for varying τ are considered for removing specular highlights (holes). Morphological region filling approach is used to fill holes in the image. To begin with hole filling operation, the binary image (A) is complemented. The convention adopted here is that the boundary pixels are labelled as 1. If non-boundary pixels are labelled as 0 then beginning with a point p inside the boundary a value of 1 is assigned. The following transformation fills the region with ones

$$X_k = (X_{k-1} \oplus S) \cap A^c \tag{1}$$

where $X_0 = p$; $k = 1, 2, 3, \ldots$; $\oplus$ is used for dilation of X_{k-1} by S which is defined as

$$X_{k-1} \oplus S = \{z | (\hat{S})_z \cap X_{k-1} \neq \phi\} \tag{2}$$

S is the symmetric structuring element defined as

$$\begin{bmatrix} 0 & 1 & 0 \\ 1 & 1 & 1 \\ 0 & 1 & 0 \end{bmatrix}$$

This algorithm terminates at k^{th} iteration if $X_k = X_{k-1}$. The image generated from last iteration X_k is combined with A using bitwise OR that contains the boundary filled image.

Each hole filled image is used to find the no. of connected components (η). η changes for change in value of threshold as shown in Figure 2. The value of threshold corresponding to minimum non-zero η is chosen as adaptive binarization threshold. However, if the minimum non-zero η occurs for more than one thresholds (as shown in Figure 2), then maximum threshold amongst them is chosen as adaptive threshold. The reason behind finding maximum amongst potential thresholds is that pupil boundary may contain some intensity values which may not contribute to connected component of pupil for lower thresholds. Figure 3 shows binary images obtained for change in τ. Algorithm 1 describes steps involved.

Algorithm 1 Adaptive_Thresholding

Require: I: Intensity Image, S: Structuring element
Ensure: B: Binary Image
  $low_\tau \Leftarrow 0.10$
  $high_\tau \Leftarrow 0.50$
  $step_\tau \Leftarrow 0.05$
  $[r\ c] :=$ size(I) {Compute width and height of image}
  for $\tau := low_\tau$ to $high_\tau$ step $step_\tau$ **do**
    $A :=$ binary(I, τ) {Image Binarisation using τ}
    $C := A^c$ {Complement of an image}
    $X_0 :=$ zeros(r, c) {Image with all zeros}
    $X_0(p) = 1$ {p is a point inside hole}
    $k \Leftarrow 0$
    repeat
      $k \Leftarrow k + 1$
      $X_k \Leftarrow (X_{k-1} \oplus S) \cap C$
    until $X_k \neq X_{k-1}$
    $H_\tau \Leftarrow X_k \cup A$ {Hole filled image}
    $\eta_\tau :=$ connComp(H_τ) {Find no. of connected components}
  end for
  $pos :=$ min_nonzero(η){Find index of minimum non-zero}
  $B \Leftarrow H_{pos}$

2.2 Pupil Detection

In traditional iris recognition systems, combination of edge detection and Circular Hough Transformation (CHT) is used for finding pupil and iris boundaries [3]. The major drawback of Hough transform is that it requires range of radius as input from the user. Further, Hough works in R^3 parameter space (number of parameters needed to describe the shape of a circle) which implies high time complexity of the transform. Hence, an efficient spectrum based approach is used for pupil detection that performs faster compared to Hough transformation without any priori estimation of radius.

In this approach, the binarised image is re-complemented to detect center of pupil. The distance of every pixel in the binary image is obtained with nearest non-zero pixel [4]. By computing the distance between pixels, spectrum showing largest filled circle can be formed within the set of foreground pixels. Since pupil is the largest filled circle in the image, the overall intensity of this spectrum is maximum at the center. The spectrum image is shown in Figure 4(a). Thus, the position of maximum value in the spectrum image is pupil center. To compute the pupil radius, an edge map of the hole filled binary image is obtained as shown in Figure 4(b). In the edge map, the distance from the detected pupil center to the nearest non-zero pixel is the pupil radius (r_p). The pupil detected image is shown in Figure 4(c). The algorithm for detecting pupil center and radius is given in Algorithm 2.

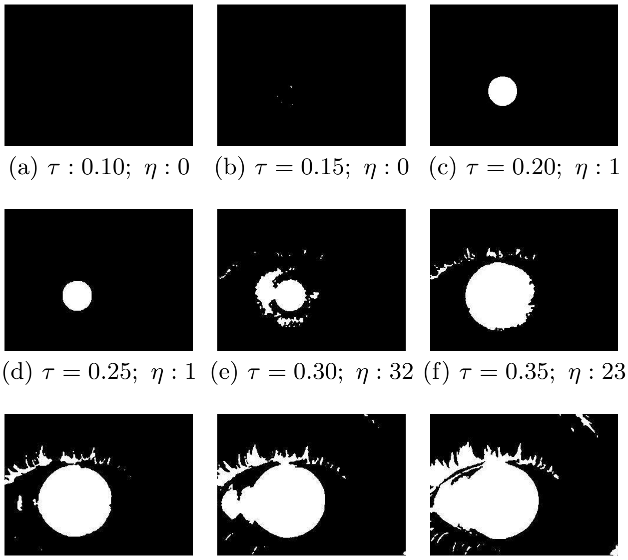

(a) $\tau : 0.10;\ \eta : 0$ (b) $\tau = 0.15;\ \eta : 0$ (c) $\tau = 0.20;\ \eta : 1$

(d) $\tau = 0.25;\ \eta : 1$ (e) $\tau = 0.30;\ \eta : 32$ (f) $\tau = 0.35;\ \eta : 23$

(g) $\tau = 0.40;\ \eta : 18$ (h) $\tau = 0.45;\ \eta : 23$ (i) $\tau = 0.50;\ \eta : 30$

Figure 3: Binary images obtained for change in threshold (τ) and number of connected components (η)

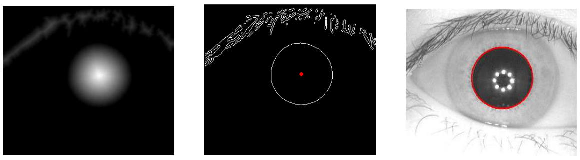

(a) (b) (c)

Figure 4: Pupil Detection: (a) Spectrum image, (b) Edge detected image and (c) Pupil localised image

2.3 Iris detection

For iris boundary detection, circular summation of intensity approach is used as proposed in [5]. The original grayscale image is blurred using median filter to remove external noise. After filtering, the contrast of image is enhanced to have sharp variation at image boundaries using histogram equalisation as shown in Figure 5(a). This contrast enhanced image is used for finding the outer iris boundary by drawing concentric circles (Figure 5(b) shows an example) of different radii from the pupil center and the intensities lying over the perimeter of the circle are summed up. Among the candidate iris circles, the circle having maximum change in intensity with respect to the previous drawn circle is the iris outer boundary as shown in Figure 5(c).

3. EXPERIMENTAL RESULTS

The proposed system has been tested on two publicly available databases BATH [6] and CASIA V3 [7].

From experimental analysis it has been observed that the system is capable of handling unconstrained scenarios as well. To mention a few, it possesses invariance to noisy instances viz. occlusion, specular highlights, person wearing contact lens, change in illumination and viewpoint (non-centered gaze). Performance accuracy of the detector is supported with the help of few illustrations. The nomenclature

Algorithm 2 Pupil_Detection

Require: B: Binary Image
Ensure: x_c: xcenter of pupil, y_c: ycenter of pupil, r_p: Radius of pupil
  $C \Leftarrow B^c$ {Complement the binary image}
  $[x\ y] :=$ find$(C == 1)$ {Find location of ones in an image}
  $l :=$ length(x) {To find the no. of elements in an array}
  for $i := 1$ to r **do**
    for $j := 1$ to c **do**
      for $k := 1$ to l **do**
        $D_k \Leftarrow \sqrt{(x_k - i)^2 + (y_k - j)^2}$
      end for
      $S_{i,j} := \min(D)$ {Minimum value of D}
    end for
  end for
  $[x_c\ y_c] \Leftarrow \max(S)$
  $E :=$ edge(C) {Edge detection}
  $j \Leftarrow y_c$ {Estimation of pupil radius}
  $r_p \Leftarrow 0$
  while $E_{x_c,j} \neq 1$ **do**
    $r_p \Leftarrow r_p + 1$
    $j \Leftarrow j + 1$
  end while

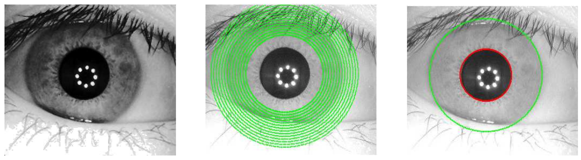

(a) (b) (c)

Figure 5: Iris Detection: (a) Contrast enhanced image, (b) Concentric circles of different radii and (c) Iris localised image

of the images are defined as *Database/Subject ID/Eye/Image Instance* (e.g. C/224/L/05).

Figure 6(a) depicts robustness against occlusion and specular highlights. It is evident that the proposed scheme performs well for higher degree of occlusion (C/010/R/04) where image is occluded by upper eyelid and the region of interest (iris) is partially outside. Further, an example showing the subject wearing contact lens is shown in Figure 6(b). The segmentation takes place accurately despite unconstrained nature of the instances.

Similarly, the system is proficient in performing against illumination variation. Change in illumination leads to dilation and contraction of pupil. Static threshold may fail to perform due to intensity variation. Samples from BATH and CASIA databases are shown in Figure 7. The localisation accuracy of the proposed system is compared against circular Hough transform [8] as shown in Table 1. The proposed system performs with an accuracy of 99.07% and 95.76% on BATH and CASIA respectively (with an average accuracy of 97.42%). Hough transform performs equally well (average accuracy of 97.35%) but localisation time for the proposed system is relatively low compared to Hough transform.

Few test cases where proposed approach outperforms Hough transformation are shown in Figure 8. To determine computation efficiency, time taken to perform segmentation is computed using 2.81GHz AMD Athlon 64 X2 Dual Core

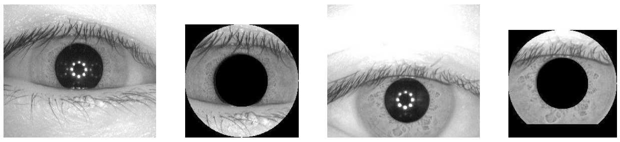

C/139/R/03 C/010/R/04

(a) Occlusion and specular highlights

C/147/R/04

(b) Subject wearing contact lens

Figure 6: Localization performance of the proposed approach for (a) occlusion and specular highlights and (b) contact lens

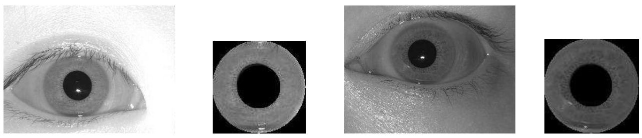

B/0017/L/10 B/0018/L/20

(a) BATH

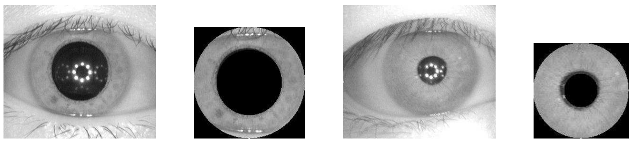

C/063/R/07 C/166/R/04

(b) CASIA

Figure 7: Localization performance of the proposed system for variation in illumination

processor with 2GB RAM. Time required to perform localisation by the proposed approach is significantly low compared to Hough transform as given in Table 2. Average time taken by the proposed approach is 0.37 seconds/image whereas Hough takes 7.68 seconds/image. From the results it is evident that system is capable of performing segmentation for unconstrained scenarios in significantly less time.

4. CONCLUSIONS

In this paper, issues owing to non-cooperative images have been addressed. An adaptive threshold is computed using no. of connected components. Pupil boundary is obtained from the binary image using spectrum approach. This approach has been tested on BATH and CASIA databases and compared against Hough transform. It has been observed that the proposed approach performs with an average accuracy of 97.42% in comparison to Hough which performs with an average accuracy of 97.35%. Though there is minor improvement in accuracy, the time required to perform segmentation reduces to 0.37 seconds/image in comparison to 7.68 seconds/image for Hough transform. This marks suitability of proposed approach for time constrained systems.

Table 1: Accuracy (in %) for the proposed approach and Hough transform

Databases → Approach ↓	**BATH**	**CASIA**
Hough [8]	99.53	95.17
Proposed	99.07	95.76

Table 2: Time taken (in seconds) for the proposed approach and Hough transform

Databases → Approach ↓	**BATH**	**CASIA**
Hough [8]	02.2820	13.0676
Proposed	00.3383	00.3960

5. REFERENCES

[1] J. Daugman. The importance of being random: statistical principles of iris recognition. *Pattern Recognition*, 36(2):279 – 291, 2003.

[2] G. Xu, Z.F. Zhang, and Y.D. Ma. Automatic iris segmentation based on local areas. In *International Conference on Pattern Recognition*, volume 4, pages 505–508. IEEE Computer Society, 2006.

[3] Q. Tian, Q. Pan, Y. Cheng, and Q. Gao. Fast algorithm and application of hough transform in iris segmentation. In *International Conference on Machine Learning and Cybernetics*, volume 7, pages 3977–3980, 2004.

[4] B. Lipinski. Iris recognition: Detecting the pupil. Connexions website, 2004. http://cnx.org/content/m12487/1.4/.

[5] L. Ma, T. Tan, Y. Wang, and D. Zhang. Efficient iris recognition by characterizing key local variations. *IEEE Transactions on Image Processing*, 13(6):739–750, 2004.

[6] BATH University Database. `http://www.bath.ac.uk/elec-eng/research/sipg/irisweb`.

[7] CASIA Database. `http://www.cbsr.ia.ac.cn/english/IrisDatabase.asp`.

[8] R.P. Wildes. Iris recognition: an emerging biometric technology. *Proceedings of the IEEE*, 85(9):1348–1363, 1997.

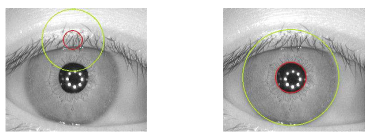

C/124/R/06

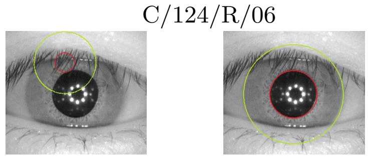

C/144/R/03

Figure 8: Sample instances where proposed approach (right) outperforms Hough transform (left)